Photodetachment of atomic negative ions near threshold in a magnetic field

D. J. Larson and R. Stoneman
Department of Physics, University of Virginia, Charlottesville, Virginia 22901
(Received 28 September 1984)

The effect of final-state interactions on the photodetachment cross section of negative ions in a magnetic field is discussed. Experiments on the location of the $^2P_{3/2}$ threshold in S^- as a function of magnetic field show clearly the effect of the zero-point energy of an electron in a magnetic field. The experiments also give a precise value for the electron affinity and provide information about the interaction between the atom and the detached electron.

I. INTRODUCTION

Experiments on photodetachment of negative ions in a magnetic field have provided information relevant to problems of electron-atom scattering in magnetic fields which are anticipated to be of importance to plasma physics and astrophysics as well as being an interesting aspect of basic atomic physics. The first theoretical description of the photodetachment process in a magnetic field[1] ignored the final-state interaction and gave reasonably good agreement with the data. Recently, new calculations have suggested that the electron-atom interaction, including that due to the atomic polarizability, modifies the electron motion in the direction perpendicular to the magnetic field enough to have a significant effect on the photodetachment cross section.[2] In this paper, we discuss the effects of the electron-atom interaction on the photodetachment cross section and present new data on the location of the threshold as a function of magnetic field. This data provides information about the effects of the electron-atom interaction.

II. DESCRIPTION OF THE PHOTODETACHMENT PROCESS

Photodetachment near threshold in the absence of magnetic fields is accurately described by the "Wigner-law" behavior, $\sigma \propto k^{2l+1}$, where k is the momentum and l the angular momentum in the final state.[3,4] This can be readily understood in terms of the golden rule, $\sigma \propto |M|^2 \rho(E)$, where if we assume that there is no interaction between the electron and the neutral in the final state, the transition matrix element M is proportional to k^l for long-wavelength electrons ($1/k \gg a_0$) and the density of states $\rho(E)$ is also proportional to k, where a_0 is the Bohr radius, giving $\sigma \propto k^{2l+1}$. As first pointed out by Wigner and later amplified by O'Malley,[5] this behavior is obtained even in the presence of a final-state interaction as long as it falls off faster than r^{-2}. Thus the centrifugal potential is the weakest potential which can change the asymptotic behavior. Shorter-range potentials can affect the size of the region over which the threshold law is valid, but do not change its form. Since our experiments deal with S^- where the electron is detached from a p orbital, either s- or d-wave final states are possible. However, near threshold only the s-wave contribution is significant, as shown explicitly by the Wigner law. The d-wave contribution is very small near threshold since for low energies the electron orbit must have a substantial radius in order to have two units of angular momentum and there is thus little overlap with the initial negative ion state. For detachment into s waves, the threshold behavior comes about because for these penetrating orbits the matrix element is first-order independent of energy and the density of states rises proportional to k.

The application of a magnetic field modifies the photodetachment cross section since the electrons are then not free to move off in three-dimensional continuum states but are constrained to cyclotron orbits. If we assume that there is no final-state interaction, the effect is that for each Landau level, there is only a one-dimensional continuum (due to motion along the direction of the magnetic field). Again only the penetrating orbits (those corresponding to zero angular momentum about the magnetic field axis) contribute significantly. Each level, independent of energy, has equal cross section but of course each level has a different threshold given by $h\nu = h\nu_0 + (n+1/2)\hbar\omega_H$ where ν is the light frequency, ν_0 is the zero-magnetic-field threshold, n is the principal quantum number of the Landau level and ω_H is the cyclotron frequency. Thus the electron affinity, defined as the energy between the ground state of the negative ion and the ground state of the neutral atom plus a free electron is changed by an amount $\frac{1}{2}\hbar\omega_H$ due to the zero-point energy of the electron in the cyclotron orbit. Also there appears a series of thresholds, one for each Landau level, and the cross section at each threshold is proportional to the density of states, which for one dimension goes as $1/k$. If the magnetic field is turned down to the point where the cyclotron spacing is less than the experimental cross-section's resolution, the sum over the individual cyclotron levels results in a Wigner-law threshold.

This description, when coupled with a calculation of the strengths and positions of the unresolved thresholds for Zeeman sublevels and when augmented by a calculation of the effects of Doppler and motional Stark broadening, produces curves which are in rather good agreement with experimental data.[1] The resolution of the experiments reported in this paper, as well as the earlier ones reported in Refs. 1 and 6, is limited by the Doppler

and motional Stark broadening. An example of a least-squares fit of this theory to recent data is shown in Fig. 1. Such fits are used to extract values for the photodetachment threshold as described in Sec. III.

An obvious limitation of the description given above is that it fails to include any final-state interaction. As pointed out by Clark[2] and as we shall see presently, a short-range final-state interaction significantly modifies the threshold behavior. This is unlike the situation in the absence of the magnetic field described above where we noted that the threshold behavior is not affected by any interaction potential that falls off faster than $1/r^2$. This difference is directly related to the well-known difference in the number of bound states in shallow potentials in different dimensions. An attractive potential always has at least one bound state in one dimension (and in two dimensions as well) but if sufficiently shallow, will not have any bound states in three dimensions. (This occurs because a particle can be bound without being localized in one dimension but not in three.) The presence of the magnetic field insures that sufficiently close to threshold, i.e., for $h\nu - h\nu_0 < \frac{3}{2}\hbar\omega_H$, the photodetachment process becomes effectively one dimensional because the motion in directions perpendicular to the magnetic field will be constrained by the field.

In order to make this more explicit, consider the addition of a short-range final-state interaction to the model for photodetachment in the presence of a magnetic field. Consider first a potential of the form

$$U(\mathbf{r}) = -U_0 a_0^3 \delta(\mathbf{r}) \ . \tag{1}$$

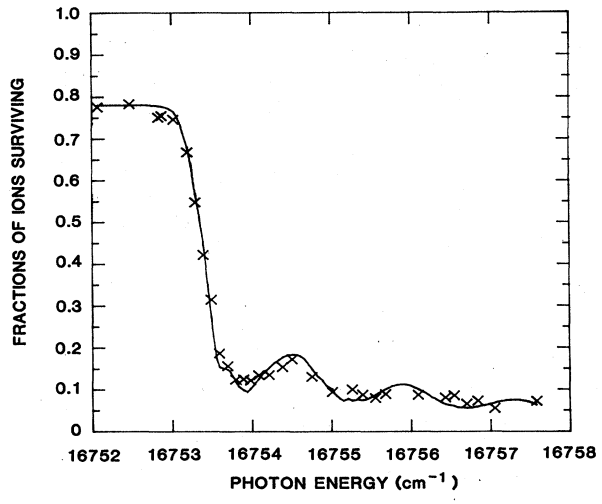

FIG. 1. Photodetachment data at 1.49 T using π-polarized light. The data points are plotted as a function of laser frequency together with a fitted curve based on the theory described in Ref. 1 and discussed in the text. The fraction surviving is less than unity even below the threshold for detachment from the $^2P_{3/2}$ state due to detachment from the $^2P_{1/2}$ state and other loss such as reaction with background gas. The fitted curve is used to obtain a value for the photodetachment threshold. At the high detachment levels used in the experiment, this value depends primarily upon the position of the threshold for detachment to the lowest Landau level.

Here the Bohr radius a_0 is used to scale the constant U_0 so that a reasonable U_0 will be on the order of a few eV. Clearly this is not a very realistic interaction potential but the results obtained with it will apply to any sufficiently short-ranged potential as discussed below. We assume that the potential is weak enough so that the motion of the detached electron in directions perpendicular to the magnetic field (assumed to be along the z axis) is determined largely by the magnetic field. Then the wave function in cylindrical coordinates is

$$\psi(\mathbf{r}) = (2\pi)^{-1/2} R_{nm}(\rho) e^{im\phi} \chi(z) \ , \tag{2}$$

where $R_{nm}(\rho)$ is the radial cyclotron wave function. Again only the states with $m=0$ will contribute to the detachment cross section. If we write the Schrödinger equation for $\psi(\mathbf{r})$ using the potential above, assume that the solution is of the form given in Eq. (2), and integrate over the radial coordinates, we obtain an equation[7] for $\chi(z)$

$$-\frac{\hbar^2}{2M}\chi''(z) + \bar{U}(z)\chi(z) = \epsilon\chi(z) \ , \tag{3}$$

where $\epsilon = E - (n+\frac{1}{2})\hbar\omega$, E is the energy of the electron,

$$\begin{aligned}\bar{U}(z) &= \int_0^\infty U(\mathbf{r}) R_{n0}^2(\rho)\rho\, d\rho \\ &= -U_0 a_0^3 \delta(z)/a_H^2 \ ,\end{aligned} \tag{4}$$

and $a_H = \sqrt{\hbar/M\omega_H}$ is the size of the cyclotron orbit. As with all one-dimensional attractive potentials, the δ function supports a bound state[8]

$$\chi_b(z) = \sqrt{\gamma/2}\, e^{-\gamma/2|z|} \tag{5}$$

of energy $\epsilon_b = -\hbar^2\gamma^2/8M$ where $\gamma = (2M/\hbar^2)(a_0^3/a_H^2)U_0$. The even-parity continuum states are of the form[8]

$$\chi_k(z) = \frac{1}{\sqrt{2\pi}}[\cos(kz) + R(k)e^{ik|z|}] \ , \tag{6}$$

where $R(k) = i\gamma/(2|k| - i\gamma)$ and $\epsilon_k = \hbar^2k^2/2M$. We need to consider only the even-parity states since the original atomic state is of odd parity. The cross section for detachment is then given by

$$\sigma \propto \int |\langle i|r|f\rangle|^2 \delta(E_f - E_i - h\nu) dE_f \ . \tag{7}$$

Near threshold $ka_0 \ll 1$ and for laboratory fields $a_0 \ll a_H$ so if we assume the initial state has a size on the order of a_0 there is significant overlap with the final state only in the region where $R_{n0}(\rho) \approx R_{n0}(0)$ and $\chi_k(z) \approx [1+R(k)]/\sqrt{2\pi}$, giving

$$\sigma(k) \propto \frac{4k}{\gamma^2 + 4k^2} \ . \tag{8}$$

This same cross section is found at each Landau threshold, independent of n. The cross section is clearly different than the $\sigma \propto 1/k$ cross section used in Ref. 1 to describe the case with no final-state interaction but it reproduces that cross section in the limit as $U_0 \to 0$ ($\gamma \to 0$). The present cross section rises from threshold proportional to k (as Clark[2] pointed out it must) but turns over and falls as $1/k$ for $k \gg \gamma$. The integrated cross section differs from the integrated $1/k$ cross section by an

amount equal to the cross section for transitions to the bound state. (That is, the bound state at $\epsilon=-\hbar^2\gamma^2/8M$ draws its oscillator strength from the continuum over a comparable energy range above threshold.) Of course for $n>0$ the "bound states" are actually resonances in the continua associated with the lower Landau levels.

If we assume a value for U_0 on the order of an eV, we find $\epsilon/h\approx 10^6$ Hz which is well below the Doppler-limited linewidth of about 3×10^9 Hz in the present experiments. Thus while the cross section in the presence of the short-range final-state interaction exhibits different threshold behavior, this difference is not discernable in present experiments and it is not surprising that the description given by Blumberg, Itano, and Larson[1] does a very reasonable job of describing the data.

Clearly the description given above is only a greatly simplified approximation to the real physical problem. However, any short-range interaction will produce a similar effect at sufficiently low magnetic field. If the interaction falls off faster than $1/r^2$, one can always choose a magnetic field such that the motion of the electron in the first Landau level is primarily determined by the magnetic field. This corresponds to choosing a field such that $U(a_H)\ll\hbar\omega_H$. In this limit, which applies to present laboratory fields and realistic electron-atom interactions (e.g., including polarizability in the e^--S interaction), the effect of the potential on the electron motion along the magnetic field and thus on the shape of the detachment cross section should be reasonably represented by Eq. (9) where $\gamma=(2M/\hbar^2a_H^2)\int U(\mathbf{r})dV$. Thus, given the resolution of the present experiments, the $\sigma\propto 1/k$ model is a reasonable approximation. In very strong magnetic fields where $a_H\approx a_0$, one will clearly have a case of strong field mixing analogous to the problem of photoionization near threshold in a magnetic field. We are thus led to the somewhat strange sounding conclusion that magnetic field effects will dominate in the limit of weak magnetic fields and that other interactions must be included as the strength of the field is increased.

In the discussion above, we have neglected the effect of the (possibly strong) short-range interaction on the motion of the electron in the directions perpendicular to the magnetic field. As suggested by Clark,[2] the situation is similar to that which gives rise to quantum defects in multielectron atoms. The electron moves under the influence of the magnetic field through most of its orbit, but then scatters off a central core, producing a phase shift and a corresponding shift in the energy levels. This means that the energy of the nth resonance should be of the form

$$E_n=\hbar\omega_H(n-\mu+\tfrac{1}{2}) \tag{9}$$

for $m=0$, where μ is the quantum defect. Clark used a numerical calculation to estimate μ for S^- at 1.07 T and found that μ should be on the order of -0.1 and should vary slowly with n. Presumably, just as in the alkali-metal atoms, μ will be a strong function of m but the calculation and the present experiments only involve $m=0$. This calculation provided the motivation for the present measurements of the absolute position of the $n=0$ thresholds (or resonances) in S^- as a function of magnetic field.

III. EXPERIMENTAL TECHNIQUE

We measured the threshold for photodetachment from negative sulfur ions in the presence of a magnetic field by observing the depletion of a cloud of S^- ions held in a Penning ion trap when the ions were illuminated with light from a tunable dye laser. This is the same basic technique used in the experiments described in Ref. 6 and analyzed in Ref. 1. A schematic diagram of the apparatus is shown in Fig. 2.

The S^- ions are created by dissociative attachment. A 300-nA beam of electrons with an energy of about 2 eV is directed through the trap while carbonyl sulfide gas at a pressure of about 3×10^{-8} Torr is fed in through a variable leak. After a few seconds the electron beam is turned off and the gas pressure is reduced to less than 4×10^{-9} Torr. Reducing the gas pressure increases the S^- lifetime which is otherwise limited to a few seconds by reaction with the carbonyl sulfide.

The number of ions in the trap is measured by driving the axial motion, typically set at 185 kHz by using a trapping potential of 3.8 V. The axial motion is driven by applying an rf voltage across the end caps of the trap. The driven ion motion is detected by measuring the current induced on the ring electrode at twice the driving frequency. This current is developed into a voltage across a tuned coil and the voltage is amplified, rectified, and detected. The number of ions is measured both before and after photodetachment in order to reduce the effect of fluctuations in the number of ions created in each cycle of the experiment.

The ions are photodetached with light from a tunable dye laser. The light is produced by a noncommercial ring dye laser tuned with a birefringent filter and two solid etalons. The laser oscillates with sufficient stability on a single axial mode without any active amplitude or frequency stabilization. Typically the laser produces about 200 mW near the S^- threshold at about 16753 cm^{-1}. Approximately half the light is directed through holes in the ring electrode of the trap. The amount of light sent through the trap is measured by a photodiode and a

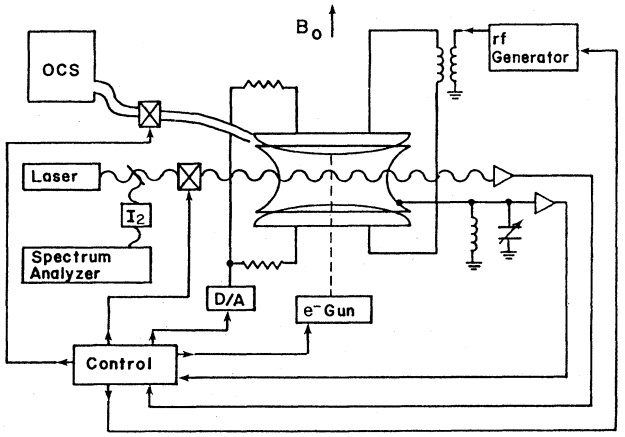

FIG. 2. Schematic diagram of the experimental apparatus. The three electrodes of the ion trap are shown together with other essential parts of the apparatus.

shutter is controlled to keep the integrated light intensity constant from cycle to cycle. The absolute frequency of the light is measured to within 0.5 GHz or better by using a Fabry-Perot spectrum analyzer together with observation of absorptions in a molecular iodine cell. Since the light is directed through the trap in a direction perpendicular to the magnetic field, measurements can be and were taken with both σ and π polarizations.

The complete data cycle consists of a sequence of filling the trap, waiting for a second or so, driving the ions to determine their number, turning on the light to photodetach, driving the ions to again measure their number, and emptying the trap. The whole cycle takes on the order of 30 s. Typically five cycles were completed at each laser frequency before changing the frequency. The laser frequency was changed in steps of about 3 GHz. We thus obtain a measure of the fraction of the number of ions which survive illumination by light of a given frequency as a function of laser frequency. In these measurements the integrated light flux through the trap was chosen to give a large detachment ratio at the threshold for detachment to the $n=0$ state of the detached electron in the magnetic field. Examples of the data are shown in Figs. 1 and 3.

In order to obtain a result for the threshold for each set of data the data points are fit to a curve based on the theory of Ref. 1 which neglects any final-state interaction. The fit parameters include electron affinity, integrated laser intensity, temperature, and the fraction of ions surviving below the threshold for detachment from the $^2P_{3/2}$ state. Magnetic field and light polarization are input as fixed parameters. The steep portion of the curve (which largely determines the fitted electron affinity) consists of a number of unresolved thresholds for the various Zeeman sublevels. The cross sections associated with each of these thresholds are weighted according to the angular momentum weights for transitions to a continuum s-wave state. Since the size of the atom is small compared to the cyclotron radius, this appears to be a reasonable approximation.

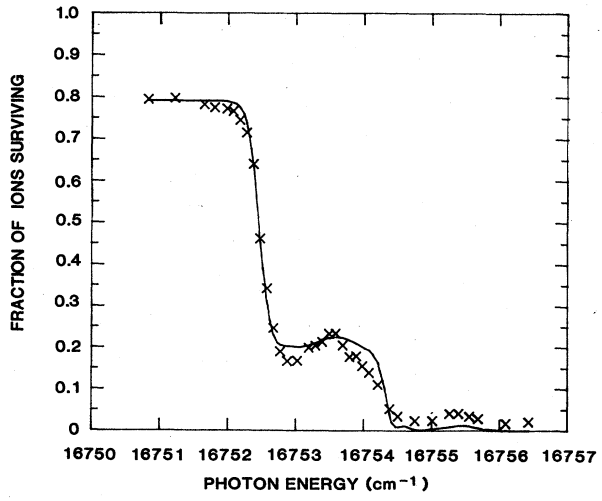

FIG. 3. Photodetachment data at 1.49 T using σ-polarized light (see Fig. 1 caption).

IV. RESULTS AND DISCUSSION

A total of eight runs at five different magnetic fields were made. Three of these were done with π polarization and five with σ. The fit to the data from each run produced a value for the electron affinity with a typical predicted error of 0.03 cm^{-1}. These values are plotted as a function of magnetic field in Fig. 4. The Zeeman structure of the ion and atom plus electron has been taken into account for each point, leaving the zero-point energy of the cyclotron levels as the primary reason for the obvious magnetic field dependence. If we assume that any correction to the apparent threshold position is linear in the magnetic field (such as due to a quantum defect which is independent of magnetic field) or small enough to be insignificant, then the data should fit a straight line with the intercept giving a value for the zero-field electron affinity. The line shown in Fig. 4 is the result of such a fit with all data points weighted equally. This line has an intercept corresponding to an electron affinity of 16 752.967(29) cm^{-1}. The slope is 0.494(24) cm^{-1}/T corresponding to an energy of $0.529(26)\hbar\omega_H$. The fit shows a scatter in the individual points on the order of 0.02 cm^{-1}, consistent with that estimated from the fits to the threshold data. There is no indication of a nonlinear dependence of the threshold upon the magnetic field. The value for the zero-magnetic-field electron affinity is remarkably close to the value 16 752.966(10) recently measured by Mead, Lykke, and Lineberger.[9]

Instead of simply comparing our result for the electron affinity to that of Mead, Lykke, and Lineberger, we can use their result as a data point in the straight-line fit. Since their value is virtually identical to ours, this will simply reduce the predicted errors in the slope and inter-

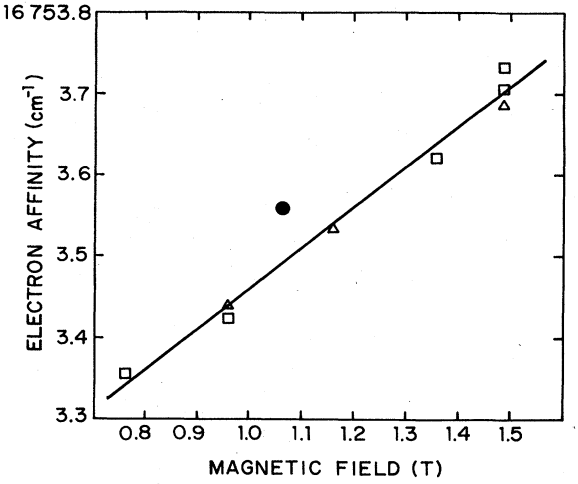

FIG. 4. Measured electron affinity as a function of magnetic field. The individual points are obtained from the fits to the data such as that shown in Figs. 1 and 3. The points for σ polarization are shown with open squares, those for π polarization with open triangles, and the value calculated by Clark (Ref. 2) by a solid circle. The intercept of the line fitted to the experimental points gives a value for the zero-magnetic-field affinity and this value is used to locate the theoretical point on the graph.

cept. Because their data point serves to decorrelate the slope and intercept, the errors predicted for these parameters will depend rather strongly on the relative weights given to the data points. The most reasonable procedure seems to be to assign an error of 0.02 cm^{-1} to our seven points and use Mead, Lykke, and Lineberger's error of 0.01 cm^{-1} for their point. The result is an electron affinity of 16752.966(8) cm^{-1} and a slope of 0.494(8) cm^{-1}/T which corresponds to an energy of $[0.529(9)]\hbar\omega_H$. This slope is three standard deviations from the slope due to zero-point energy and shows a displacement in the direction predicted by Clark. The data is, however, clearly not in agreement with Clark's estimate for the shift at 1.07 T. Using the measured value for the electron affinity, we can put Clark's prediction on our plot. It corresponds to an energy of $0.593\hbar\omega_H$. The solid circle in Fig. 4 shows the result.

One serious question about the procedure used to obtain the results above is in the use of an approximate model to extract results for the electron affinity. The experiments clearly have the sensitivity to find the thresholds to within at least 0.02 cm^{-1} but the derived location of the threshold may depend (in a field-dependent way) upon assumptions about the weighting of the various unresolved Zeeman thresholds. Comparing Figs. 1 and 3 shows that the observed thresholds for σ and π polarization differ by approximately 1 cm^{-1} at 1.49 T. A bizarre distribution of threshold weights could cause relative shifts between the σ- and π-derived thresholds by an appreciable fraction of this 1 cm^{-1}. In view of this, an indication of different behavior for σ and π polarizations may be important. This is suggested by the curves in Figs. 1 and 3 and borne out by the other data. There is a tendency for the data taken with π polarization to fit the model better than that taken with σ polarization. The model tends to understate the oscillations observed with σ polarization.

On the other hand, there are substantial and rather direct, although only semiquantitative confirmations of the weighting factors. One is provided by the rather good agreement between the model and the photodetachment data taken with lower integrated light intensities (see Ref. 1). In particular, the presence and location of a second maximum in the curve for σ polarization depends upon the particular weighting factors used for the various Zeeman thresholds. Even giving equal weight to all Zeeman thresholds, which would shift the derived threshold by something on the order of 0.06 cm^{-1} at 1.49 T, is clearly ruled out because it would virtually eliminate the observed second maximum. A second source of confirmation is the observed strength of microwave-driven Zeeman transitions after state selection using photodetachment by light of appropriate frequency and polarization.[10] In particular, the observation of transitions from the $m_J=-\frac{3}{2}$ state, but not from the $m_J=+\frac{3}{2}$ state, after state selection by σ-polarized light with photon energy between $h\nu_0$ and $h\nu_0+\frac{1}{2}h\omega_H$, also supports the predicted weighting factors. Finally, and most significantly, fitting the present results for σ polarization together with the zero-field result of Mead, Lykke, and Lineberger gives a slope of 0.498(10) cm^{-1}/T which is consistent with the slope of 0.487(5) cm^{-1}/T obtained using the points for π polarization plus the zero-field result. This is not a clear confirmation of the weighting factors since under the conditions of high light intensity used in these experiments the fitted threshold positions become somewhat insensitive to the weighting factors, but is support for the correctness of the slope derived from the fitted positions since it seems very unlikely that any errors in the quite different weights for σ and π polarization would be just such as to give identical but incorrect results for threshold positions.

V. CONCLUSIONS

Extensions of the model of Blumberg, Itano, and Larson[1] used to describe photodetachment in a magnetic field have been discussed. For present experimental conditions it appears to give reasonable results. The electron affinity of S^- ions has been measured in experiments at various magnetic fields, giving a result of 16752.967(29) cm^{-1} for the electron affinity at zero magnetic field or 16752.966(8) cm^{-1} when data from an independent measurement by Mead, Lykke, and Lineberger[9] is included. The zero-point energy of an electron in a magnetic field has been observed directly through its effect on the threshold for photodetachment from a negative ion. There is a strong indication in the data that a shift of the sort proposed by Clark[2] does occur but any such shift must be clearly less than that estimated by Clark. Finally, there are some slight suggestions in the data of a difference between photodetachment with σ and π polarizations which has not been accounted for in the model. Photodetachment experiments using some combination of higher magnetic fields, different ions, cooler ions, and state selection could provide significant new data about such effects.

ACKNOWLEDGMENTS

This work was supported by the U.S. Office of Naval Research and by the National Science Foundation.

[1]W. A. M. Blumberg, W. M. Itano, and D. J. Larson, Phys. Rev. A **19**, 139 (1979).
[2]C. W. Clark, Phys. Rev. A **28**, 83 (1983).
[3]E. P. Wigner, Phys. Rev. **73**, 1002 (1948).
[4]H. Hotop, T. A. Patterson, and W. C. Lineberger, Phys. Rev. A **8**, 762 (1973).
[5]T. F. O'Malley, Phys. Rev. **137**, A1668 (1965).
[6]W. A. M. Blumberg, R. M. Jopson, and D. J. Larson, Phys. Rev. Lett. **40**, 1320 (1978).
[7]L. D. Landau and E. M. Lifshitz, *Quantum Mechanics: Non-Relativistic Theory*, 3rd ed. (Addison-Wesley, Reading, Mass., 1977), pp. 456–460.
[8]K. Gottfried, *Quantum Mechanics* (Benjamin, New York, 1966), p. 50–52.
[9]R. D. Mead, K. R. Lykke, and W. C. Lineberger (private communication).
[10]R. M. Jopson and D. J. Larson, Phys. Rev. Lett. **47**, 789 (1981).